UPPER BOUND ON THE HIGGS MASS

ANNA HASENFRATZ
Department of Physics, University of Arizona
Tucson, AZ-85721

ABSTRACT

The scalar Higgs boson is the most intriguing, still missing part of the electroweak Standard Model. Though its mass is a free parameter of the theory, the consistency of the effective model restricts its value. Recent lattice calculations estimate an upper bound for the Higgs mass around $650GeV$. This review summarizes the different techniques leading to this value and discusses some of the conceptual problems of the calculations.

1. Introduction

The minimal Standard Model of electroweak interactions describes the low and medium energy data exceptionally well [1]. While the Standard Model is not expected to be valid at arbitrary large energies, experimental data gives no information yet of the energy range where the model breaks down and new interactions come into play. In fact, with present experimental accuracy and energy range there is no signal for the breakdown of the Standard Model at all. Nevertheless, the Standard Model can be only a low energy effective theory, a theory with possibly large, but finite cutoff. In the infinite cut-off limit the Standard Model describes a non-interacting free field theory, it is "trivial" [2].

The success of the Standard Model is mainly due to its many perturbative properties. The $SU(2)$ gauge coupling and the Yukawa couplings (with the possible exception of the yet unknown top-quark-scalar interaction) are small not only at the physical scale, but because of asymptotic freedom, at high energies too. Despite the perturbative success of the Standard Model, one of its main building element, the scalar Higgs particle is still unknown [1]. It has not been detected experimentally nor

[1] There are attempts to formulate models without a scalar boson. However, all these models give the Standard Model as low energy effective theory with a scalar particle. In this review we do not consider these alternative high(er) energy theories but rather restrict ourselves to the low energy Standard Model and study its properties as an effective theory [3].

has its mass been predicted theoretically. The present experimental lower bound on the Higgs mass is around $50GeV$.

The Higgs particle, which is related to the renormalized scalar coupling is a free parameter of the theory. The problem we are considering in this review is the following: is the Higgs mass completely arbitrary within the Standard Model or is it restricted in any way in a physically sensible theory? Alternatively, can the low energy effective Standard Model be consistent with arbitrary renormalized scalar coupling or is λ_R restricted physically? As the scalar coupling is not asymptotically free, even if the renormalized coupling λ_R is small, the running coupling at high energies can be large. The Higgs phenomena is in general non-perturbative.

Already 1-loop perturbation theory suggests that λ_R cannot be arbitrary large [4]. Consider the scalar sector of the Standard Model and denote the bare coupling at the cut-off scale by λ_b. Let us assume for a moment that the 1-loop renormalization group β function is valid even outside the perturbative region. Then the running coupling at some energy E is

$$\lambda(E) = \frac{1}{1/\lambda_b + c\ ln(\Lambda_{cut}/E)}, \tag{1}$$

where $c = 12/8\pi^2$ for the 4-dimensional $O(4)$ scalar model without gauge or fermionic fields. At the scale of the Higgs mass

$$\lambda(m_H) \equiv \lambda_R = \frac{1}{1/\lambda_b + c\ ln(\Lambda_{cut}/m_H)}, \leq \frac{1}{c\ ln(\Lambda_{cut}/m_H)} \tag{2}$$

the upper bound corresponding to infinite bare coupling $\lambda_b = \infty$. In a physically sensible theory the cut-off should be much larger then the relevant physical energy scales. If we require, for example, $\Lambda_{cut}/m_H \geq 3\pi$, we get $\lambda(m_H) \leq 8\pi^2/12ln(3\pi)$, which implies for the ratio of the Higgs mass and vacuum condensate F_G

$$\begin{aligned} R = \frac{m_H}{F_G} = \sqrt{4\lambda(m_H)} \leq 3.4 \qquad or \\ m_H \leq 850GeV. \end{aligned} \tag{3}$$

While the above example illustrates why the Higgs particle mass is bounded in the effective Standard Model, it should not be considered more than an illustration. The obvious shortcomings are

1) The upper bound of the Higgs mass is a non-perturbative problem. It is related to how an infinitely strong bare coupling changes from the cut-off scale to physical energies. Using the 1-loop β function is only a crude approximation.

2) Requiring $\Lambda_{cut}/m_H \geq 3\pi$ is an arbitrary constraint. The cut-off is not a well defined quantity in an effective theory. A finite cut-off nevertheless has measurable, physical consequences at lower energies. Instead of fixing Λ_{cut}/m_H to an arbitrary number, one has to analyze the physical consequences of a finite cut-off. One can require that some specific physical quantity shows for example less then 1% or 5 % cut-off violation effects at the scale of the Higgs mass.

3) Whenever we are working with effective theories, we have to deal with renormalization effects. Regularization schemes can differ by finite inverse cut-off corrections and can show finite cut-off violations at different levels. Even if we require the same physical cut-off violation effects on physical amplitudes at the Higgs mass scale, different regularizations can predict different upper bound values for m_H. How much the upper bound changes within (reasonable) regularization schemes determines the universality of the upper bound calculations.

The above problems were extensively studied in recent years. In the following we will discuss different non-perturbative calculations for the upper bound problem, describe a physical way to characterize cut-off effects and consider the universality problem within certain type of regularization schemes [5].

2. The Model; Definitions and General Considerations

2.1. The role of the gauge fields

In the Standard Model the interactions between the scalar sector and the gauge fields are weak. The SU(2) and U(1) gauge couplings are small, and the effect of the strongly interacting SU(3) sector is indirect, only through the quarks via the Yukawa coupling. For light quarks the Yukawa coupling is small, the interaction is weak.

On the other hand for the upper bound problem we are interested in the strongest possible scalar coupling. We start with infinite bare coupling and study how the running coupling decreases with decreasing energy. It is expected that the small

gauge couplings will not influence the running of the scalar coupling. While some non-perturbative effect can not be completely excluded, it is a plausible assumption that the upper bound problem can be studied within the scalar sector taking the gauge fields into account perturbatively.

Without gauge interaction the lowest value of the renormalized coupling $\lambda_R = 0$, the Higgs boson can be massless. The gauge field has an important effect for the lower bound of the Higgs mass though. This problem has been extensively studied in the literature and we do not discuss it in this review [6].

2.2. MC study of coupled SU(2) gauge-scalar system

Monte Carlo studies of the SU(2) gauge-scalar system support the assumption that the gauge field is coupled perturbatively to the scalar sector.

Numerical simulations of the gauge-scalar model are rather difficult [7]. The main problem is the existence of two different mass scales, $m_H \sim 10 m_W$. If the heavy particle is light enough in lattice units that it is not distorted by lattice artifacts ($m_H a \leq 1$), the light particle is too light and distorted by finite lattice size effects on presently accessible lattices. Nevertheless numerical results from gauge-scalar system simulations are in agreement with other, better controlled calculations. The relation between the W mass and field expectation value follows the perturbative form. The predicted upper bound is about $730 GeV$.

The most important result from the full gauge-scalar calculations is the strong indication that it is indeed sufficient to handle only the scalar part of the model non-perturbatively.

2.3. Connection between the $O(4)$ model and physical quantities

We need to express m_W and m_H in terms of the $O(4)$ model observables.

The action of the continuum $O(4)$ model is

$$S_c = \int d^4x \left[\frac{1}{2} \sum_{\alpha=1}^{4} (\partial\mu\phi_\alpha)^2 + \frac{1}{2} m^2 (\sum_{\alpha=1}^{4} \phi_\alpha^2) + \frac{\lambda_c}{4} (\sum_{\alpha=1}^{4} \phi_\alpha^2)^2 - j\phi^0 \right]. \qquad (4)$$

In infinite volume the spectrum contains one massive boson and 3 massless Goldstone particles in the broken phase. The basic observables are the vacuum expectation value

and the propagators

$$\Sigma = \langle \sigma \rangle , \qquad \left\langle \phi^\alpha(p)\phi^\beta(-p) \right\rangle_c , \tag{5}$$

where we use $\phi^\alpha = (\sigma, \pi^1, \pi^2, \pi^3)$. We chose the direction of the symmetry breaking to be the first component. The wave function renormalization constant and the scalar mass is defined through the propagators

$$\begin{aligned} G_G|_{p^2\to 0} &= \left\langle \pi^i(p)\pi^j(-p) \right\rangle_{p^2\to 0} = \delta_{ij} Z_G(p^2 + O(p^4))^{-1}, \\ G_\sigma|_{p^2=\mu^2} &= \langle \sigma(p)\sigma(-p)\rangle_{p^2=\mu^2} = Z_\sigma(\mu^2 + m_H^2(\mu))^{-1}. \end{aligned} \tag{6}$$

For $\mu = O(m_H)$, $m_H(\mu)$ is close to m_H and the relation can be calculated perturbatively. Note that the σ propagator G_σ is divergent at $p^2 = 0$ due to the Goldstone contribution. The relation of the $O(4)$ observables to m_W is

$$m_W^2 = \frac{1}{4} g_2^2 F_G^2 + O(g_2^4 ln(g_2^2)), \tag{7}$$

where F_G is the Goldstone decay constant

$$F_G = Z_G^{-1/2}\Sigma. \tag{8}$$

The derivation of the above formulae can be found in the literature and we refer the reader to [8].

2.4. The lattice regularized $O(4)$ model

Most of the non-perturbative studies used the hypercubic lattice regularized version of the $O(4)$ model. The lattice action is

$$S = -\kappa \sum_{n,\mu,\alpha} \varphi_n^\alpha(\varphi_{n+\mu}^\alpha + \varphi_{n-\mu}^\alpha) + \sum_{n,\alpha} \varphi_n^\alpha \varphi_n^\alpha + \lambda \sum_n (\sum_\alpha \varphi_n^\alpha \varphi_n^\alpha - 1)^2 - J \sum_n \varphi_n^0, \tag{9}$$

where $\kappa, \lambda \geq 0$ are the bare hopping and quartic coupling parameters respectively. The external source allows the proper definition of spontaneous symmetry breaking. Its presence is essential in the use of chiral perturbation theory. The cut-off is proportional to the inverse of the only dimensional parameter, the lattice spacing a. We define the cut-off on the hypercubic lattice as $\Lambda_{cut} = \pi/a$. In the following we denote the dimensionless lattice mass by m_R, $m_R = a m_H$.

The continuum normalization is obtained by rescaling

$$\phi^\alpha a = \sqrt{2\kappa}\varphi^\alpha, \quad j a^3 = \frac{J}{\sqrt{2\kappa}}. \tag{10}$$

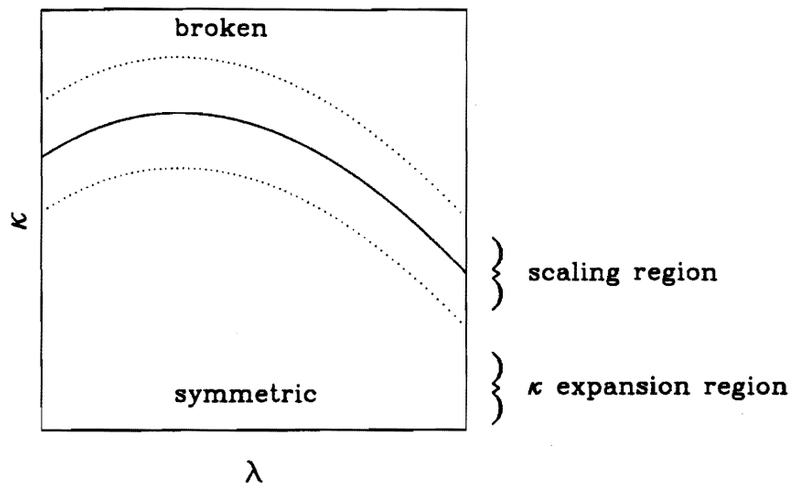

FIGURE 1

The sketch of the phase diagram of the lattice regularized $O(4)$ model

The relation between the continuum and lattice parameters are

$$m^2a^2 = \frac{1-2\lambda}{\kappa} - 8, \qquad \lambda_c = \frac{\lambda}{\kappa^2} \tag{11}$$

corresponding to the action Eq. (4).

The phase diagram of the lattice regularized model is sketched in Fig.1. The small κ phase is symmetric, separated by a second order phase transition line from the large κ broken phase. At $\lambda = 0$ the critical point is $\kappa_c = 1/8$ or $m^2a^2 = 0$, the perturbative fixed point. The infinite cutoff limit corresponds to the second order phase transition line where the dimensionless lattice mass $m_R = 0$ therefore $a = 0$. Effective theories with large but finite cut-off are described by the region around the phase transition line. The point (λ, κ) in the phase space where the dimensionless lattice mass is m_R corresponds to an effective theory with

$$\Lambda_{cut} \sim \frac{\pi}{a} = \pi\frac{m_H}{m_R}. \tag{12}$$

Triviality in this language means that no other fixed point but the perturbative Gaussian fixed point at $\lambda = 0, \kappa = 1/8$ exists. Every point of the second order phase transition surface describes the same infinite cut-off theory with $\lambda_R = 0$.

Close to the phase transition line physical observables behave in a universal way. If this scaling behavior is governed by the Gaussian fixed point, the critical exponents can be calculated perturbatively. The scaling formulae for the $O(n)$ model up to two loop level are

$$\begin{aligned} \Sigma/a &\sim \tau^{1/2}|ln|\tau||^{\frac{3}{n+8}} \quad , \\ m_R &\sim \tau^{1/2}|ln|\tau||^{-\frac{n+2}{2(n+8)}} \quad , \end{aligned} \tag{13}$$

where $\tau = \kappa - \kappa_c$. As these scaling laws are derived at the perturbative fixed point, they are obviously valid for small λ. If the theory is trivial, the same scaling formulae should be valid everywhere around the phase transition surface including $\lambda = \infty$. Scaling behavior can be used to check and understand triviality.

In the following we will discuss a few of the different methods recently used to study the broken phase of the scalar $O(4)$ model. We consider only the $\lambda_b = \infty$ case and summarize the results in an "envelope plot" showing the ratio m_H/F_G as the function of $1/m_R = \Lambda_{cut}/\pi m_H$. The symmetric phase of the model has been also extensively studied [9,10]. We do not discuss those calculations here unless they are directly related to the method used in the broken phase. There are several calculations investigating the 1-component ϕ^4 model with similar techniques. The reader is referred to the original literature [10,11].

3. Non-perturbative Studies of the $O(4)$ Model; Analytical Calculations

3.1. Approximate non-perturbative renormalization group equation

The first non-perturbative analytical estimate for the upper bound of the Higgs mass was obtained by solving the exact renormalization group equations in the local potential approximation [12]. An arbitrary $O(n)$ potential $V(\sum_{\alpha=1}^{n} \phi_\alpha^2)$ is allowed but no derivative couplings are considered. The change in the action after a renormalization group transformation $\Lambda_{cut} \to e^{-t}\Lambda_{cut}$ is projected back to the subspace without derivative couplings

$$\begin{aligned} S = \int d^dx \left[\frac{1}{2}\sum_{\alpha=1}^{n}(\partial_\mu\phi_\alpha)^2 + V(\sum_{\alpha=1}^{n}\phi_\alpha^2)\right] &\xrightarrow[\Lambda_{cut} \to e^{-t}\Lambda_{cut}]{} \\ \longrightarrow S(t) = \int d^dx \left[\frac{1}{2}\sum_{\alpha=1}^{n}(\partial_\mu\phi_\alpha)^2 + V(\sum_{\alpha=1}^{n}\phi_\alpha^2, t)\right] &. \end{aligned} \tag{14}$$

No further approximation is necessary to derive the RG equations for the potential $V(\sum_{\alpha=1}^{n}\phi_\alpha^2, t)$. The function

$$f(x/n^{1/2}, t) = n^{-1/2}\frac{\partial}{\partial x}V(x,t) \tag{15}$$

satisfies the differential equation

$$\frac{\partial f}{\partial t} = \frac{A_d}{2}\left[\frac{1}{n}\frac{f''}{1+f'} + \frac{n-1}{n}\frac{xf'-f}{x^2+xf}\right] + \left(1-\frac{d}{2}\right)xf' + \left(1+\frac{d}{2}\right)f, \tag{16}$$

where prime denotes $\partial/\partial x$, A_d is a constant ($1/8\pi^2$ for d=4) and n is the number of real scalar fields (=4).

The non-linear partial differential equation (16) can be solved numerically. From the renormalization group flow the phase diagram, fixed point structure and the critical exponents can be extracted [13]. The method predicts correctly the different fixed points in $2 < d < 4$ and gives reasonable critical exponents in $d = 3$ for the ferromagnetic fixed point. In 4 dimensions it predicts the existence of only one fixed point, the Gaussian one with correct critical exponents.

For the upper bound envelope calculation the RG equation (16) is used to run the system from the strongly coupled region to the vicinity of the Gaussian fixed point where perturbation theory can be used to connect m_H and F_G. The envelope obtained with this method is shown in Fig.2.

The local potential method cannot be improved systematically and it is not possible to estimate the error caused by the approximation. Keeping only one derivative interaction term forces the wave function renormalization constants Z_G and Z_σ to be 1. Other numerical and analytical methods predict that in the 4 dimensional $O(4)$ model both Z_G and Z_σ are close to 1, therefore it is not surprising that the envelope and upper bound obtained in the local potential approximation agrees well with those calculations.

3.2. Strong coupling expansion combined with perturbative RG

This (semi)-analytic technique covers regions with large correlation length that are outside the reach of MC calculations. Together with numerical simulations it gives a complete, controlled description of the model.

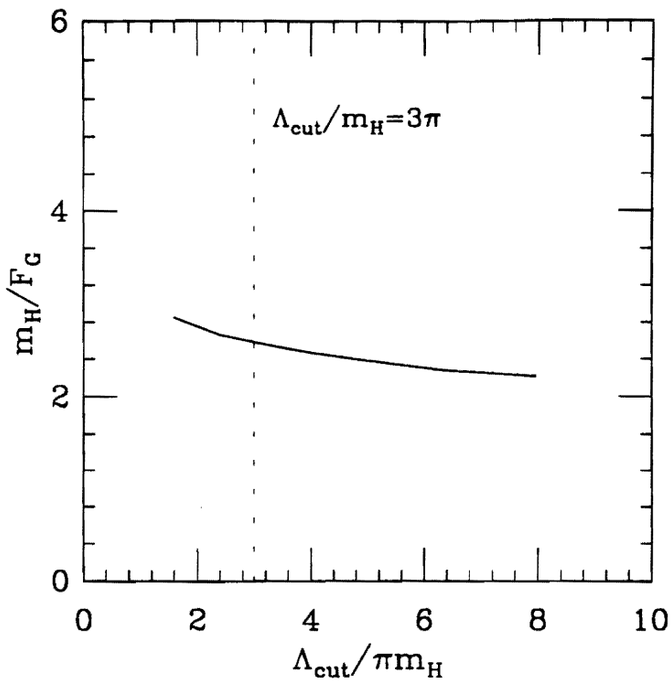

FIGURE 2

The ratio m_H/F_G as the function of the scale change $\Lambda_{cut}/\pi m_H$ for $\lambda = \infty$ as predicted by the approximate non-perturbative RG method.

The analysis is performed at a fixed, arbitrary λ. Hypercubic lattice regularization is considered. The method combines strong coupling (small κ) expansion with weak coupling (perturbative) RG equations (Fig.1.). It has been applied first to the 1-component model and later has been extended to general $O(n)$ theories [10,14].

First consider the symmetric phase. At $\kappa = 0$ the model is trivially solvable. For small κ a high order κ series (high temperature expansion) is calculated for the relevant quantities m_R, λ_R, Z_G. For example, for m_R one has

$$m_R = \frac{1}{\sqrt{\kappa}} \sum_{\nu=0}^{\infty} m_R^{(\nu)}(\lambda)\kappa^{\nu}, \tag{17}$$

where the coefficients m_R^{ν} have been calculated up to $\nu = 14$ for the $O(n)$ model. The expansion can be controlled from $m_R = \infty$ up to $m_R \approx 0.5$ corresponding to the region from $\kappa = 0$ to approximately $\kappa \leq 0.95\kappa_c$.

Around the critical region weak coupling perturbative renormalization group equations are used. The dependence of the renormalized coupling on the cut-off is described by the Callan-Symanzik β function

$$-\Lambda(\frac{\partial \lambda_R}{\partial \Lambda}) = \beta(m_R, \lambda_R), \tag{18}$$

or in lattice units

$$m_R(\frac{\partial \lambda_R}{\partial m_R}) = \beta(m_R, \lambda_R). \tag{19}$$

If we know the β function, the above equation can be integrated from the region $\kappa \approx 0.95\kappa_c$ ($m_R \approx 0.5$) up to the critical line where $m_R = 0$. The initial values for m_R and λ_R are obtained from the high temperature series.

The Callan-Symanzik β function is known up to 3 loops. Assuming that the 3-loop perturbative formula is sufficient to describe the region from $m_R = 0$ to $m_R \approx 0.5$, the combination of the two procedures will cover the whole symmetric phase.

Around the critical region where $m_R \to 0$ the renormalized coupling λ_R goes to zero as well. The dependence of m_R on the coupling is given by the formula

$$m_R = Ce^{-1/\beta_0\lambda_R}(\beta_0\lambda_R)^{-\beta_1/\beta_0^2}. \tag{20}$$

This functional dependence is valid in both the symmetric and broken phase though with different C_s and C_b coefficients. The relation between C_s and C_b can be calculated. If we define the renormalized coupling in the broken phase as

$$\lambda_R = Z_G\frac{3m_H^2}{\Sigma^2}, \tag{21}$$

we get

$$C_b = e^{1/6}C_s. \tag{22}$$

The constant C_s can be obtained by comparing the integrated Eq (19) and Eq (20). Using C_b the RG equation is used to predict m_R within the scaling region in the broken phase. Assuming the 3-loop renormalization group equation covers the region $m_R \leq 0.5$ in the broken phase too, the envelope of Fig.3. is obtained for the $O(4)$ model.

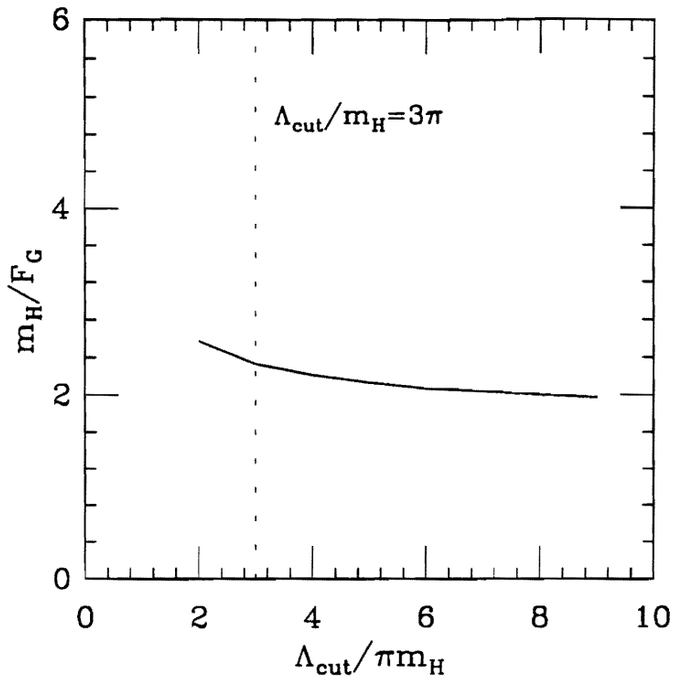

FIGURE 3

The ratio m_H/F_G as the function of the scale change $\Lambda_{cut}/\pi m_H$ for $\lambda = \infty$ as predicted by the method of Ref. [10,14].

The errors of this analysis come from the truncation of the small κ expansion, the truncation of the perturbative expansion and the propagation of those errors during the subsequent steps of the calculation.

4. Non-perturbative Studies of the $O(4)$ Model; Monte-Carlo calculations

4.1. Direct measurements

The first numerical MC calculation for the upper bound problem dates back to 1985 [15]. Since then several extensive numerical simulations for the $O(4)$ model on hypercubic lattices have been published. The methods used were occasionally quite different but the final results are in agreement [16-19].

For the upper bound problem one does not have to work at very large correlation length. It is sufficient to make the cut-off only a few times larger than the scalar

mass, which makes numerical simulations feasible. That, and the relative simplicity of the $O(4)$ model explain that these calculations are well controlled statistically and systematically as well.

On a finite lattice there is no spontaneous symmetry breaking. While in the broken phase on any given configuration the spins are ordered, the direction of the symmetry breaking rotates around in the $O(4)$ space due to tunneling between the infinite degenerate ground states. On a finite lattice the spontaneous magnetization averages to zero. The infinite volume limit can be mimiced by rotating the orientation of the spontaneous symmetry breaking to a given direction, for example the first, in every configuration. If we define

$$M^\alpha = \frac{1}{V}\sum_n \phi_n^\alpha, \tag{23}$$

the σ field operator on any given configuration is approximated as

$$\overline{\sigma}_n = \frac{\phi_n^\alpha M^\alpha}{|M|}. \tag{24}$$

The vacuum expectation value is $\Sigma = \langle\overline{\sigma}\rangle$, while $\langle\overline{\sigma}_o\overline{\sigma}_n\rangle$ gives the longitudinal propagator and m_H. The transversal components are associated with the Goldstone fields. This rotation technique introduces systematical errors in finite volume. The difference between Σ and the measured value of the projection $\langle M^\alpha\phi_x^\alpha / \mid M \mid\rangle$ is of order $V^{-\frac{1}{2}}$ and thus goes to zero as the volume goes to infinity . The volume dependence of the projected correlation function is less understood though [20-22].

We will discuss results at $\lambda = \infty$ only.

The field expectation value Σ and scalar mass m_R obtained using the rotation technique are plotted in Fig.4. The one loop scaling relation is satisfied within errors up to $m_R \sim 0.8$. This supports not only the triviality of the scalar model but shows that there is a relatively wide scaling region where physical quantities are universal.

Finally we need the Goldstone boson wave function renormalization constant. To calculate Z_G we have to investigate the Goldstone propagator. The Goldtsone bosons are massless in the infinite volume limit and light though massive in a finite box. We cannot avoid the problem of light/massless particles associated with the spontaneous symmetry breaking of a continuous symmetry any longer. Chiral

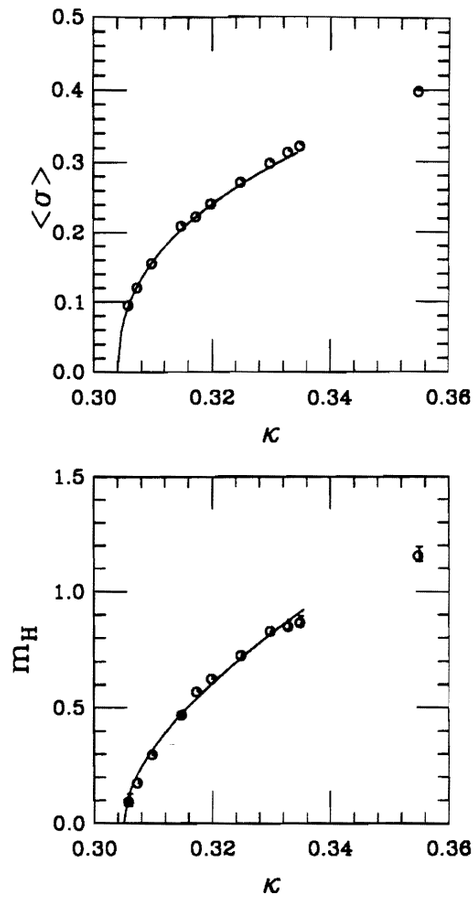

FIGURE 4

The field expectation value and the scalar mass at $\lambda = \infty$. The solid curves correspond to the 1-loop scaling formulae.

perturbation theory offers a well controlled way to describe the effects of Goldstone bosons in finite volume. Its strength is that instead of trying to avoid finite volume effects associated with the light Goldstone particles, it uses the strong dependence on finite volume and finite external source to extract infinite volume, zero external source information. Chiral perturbation theory helps not only in controlling finite size effects but it provides a theoretically correct definition for Σ and Z_G.

4.2. Finite size effects and chiral perturbation theory

The basic physical assumption behind chiral perturbation theory is easy to

formulate. The low energy behavior of a system with spontaneously broken continuous symmetry is determined by the massless (in finite volume, light) Goldstone particles and their symmetry properties. The details of the original system are unimportant as long as the massive particles are heavy compared to the Goldstone bosons and the volume is large enough so the finite size effects associated with the massive particles are negligible.

The low energy behavior can be described by an effective Lagrangean with the same symmetry properties as the original system. The couplings of this effective model depend on the low energy infinite volume physical constants of the original theory. This Lagrangean has to be simple enough to allow a systematic perturbative expansion of finite volume/finite external field quantities. This way chiral perturbation theory connects the low energy infinite volume constants to the numerically easier to measure finite volume/finite field quantities.

This theory was first applied to the finite volume, finite temperature dependence of QCD with light quarks [23]. The application for the $O(4)$ problem proved to be an exceptionally good testing ground for the applicability and accuracy of chiral perturbation theory [18]. In recent years the details of chiral perturbation theory up to 2 loop level have been worked out for a variety of statistical mechanics models in addition to the applications for QCD and the Higgs upper bound problem [20,22]. Here we summarize only the most basic formulae as applied to the $O(4)$ model.

In the following we concentrate on the finite volume effects related to the Goldstone bosons and assume that the finite size effects caused by the massive particle are negligible, $m_R << 1/L$. Consider the model with a constant, $O(4)$-symmetry breaking external source j (Eq. (4)). For small values of j, the qualitative properties of the system at large volume are controlled by the parameter $\Sigma j V$. If this parameter is small then the expectation value of the field is small and the correlation functions are approximately $O(4)$-symmetric. Holding j fixed and letting the volume grow, we eventually reach the region $\Sigma j V \gg 1$ where the expectation value of the field is approximately the same as at infinite volume. If the volume is large and the source is small, the dependence of the expectation values and correlation functions on V and on j are unambiguously determined by the symmetry properties of the model in terms of the two constants Σ and Z_G (or F_G). In the following, we show that numerical data very clearly exhibit the predicted volume dependence. This way the

extrapolation to $V = \infty, j = 0$ can be performed.

At infinite volume, the scale of the $O(4)$ symmetric system is set by the mass of the Higgs particle. In the presence of a small symmetry breaking term j, the model contains a second, independent scale, which may be identified by the mass of the Goldstone bosons, m_G. At leading order in j

$$m_G^2 = \frac{Z_G j}{\Sigma}. \tag{25}$$

The symmetry properties of the model are controlled by the mass of the Goldstone bosons if $m_G << m_H$ and the box is large compared to the Compton wave length m_H^{-1}. For a hypercube of size L^4 that means

$$j << \frac{m_H^2 \Sigma^2}{Z_G} \quad ; \quad L >> m_R^{-1}. \tag{26}$$

If the conditions (26) are met, the expectation values and correlation functions can systematically be expanded in inverse powers of L. The detailed properties of the expansion depend on the ratio of L to the Compton wavelength of the Goldstone bosons [18,20]. In the following we give formulas corresponding to small external source, i.e. for the region

$$m_G L \leq 1. \tag{27}$$

The expectation value of the field is given by a series in $1/L^2$, with coefficients that are non-trivial functions of the product jL^4. The first two terms in this series may be written in the form

$$\begin{aligned} jL^4 \left\langle \varphi_x^0 \right\rangle &= u^2 \eta(u)(1 + O(L^{-4})), \\ u &= \Sigma j L^4 (1 + \frac{r}{F_G^2 L^2}), \\ \eta(u) &= \frac{1}{u} \frac{I_2(u)}{I_1(u)}, \end{aligned} \tag{28}$$

where $I_1(u)$ and $I_2(u)$ are the standard Bessel functions of imaginary argument. The value of r depends on the shape of the box. For a symmetric hypercube, $r = 0.2107$.

For illustration Fig.5. shows $\langle \varphi^0 \rangle$ as a function of the external source j for several values of κ on $8^4, 10^4$ and 12^4 lattices [18]. The curves at any given κ correspond to a one parameter fit which determines Σ in the infinite volume, zero external

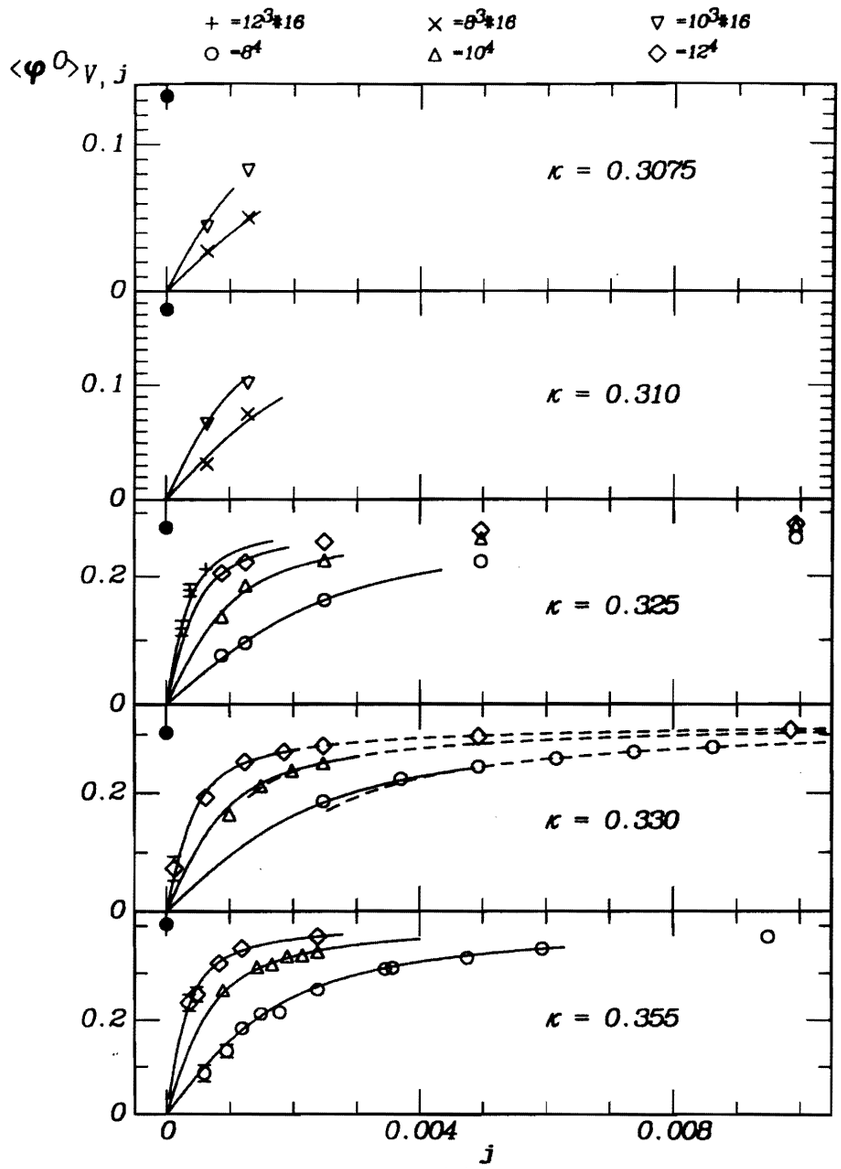

FIGURE 5

The dependence of the field expectation value on the external source on different size lattices.

field limit. The values for Σ in all cases are in complete agreement with the field expectation values obtained using the rotation technique.

The Goldstone wave function renormalization constant Z_G is extracted from

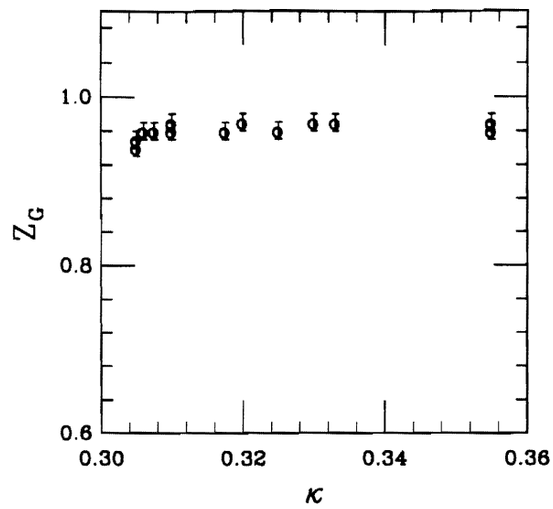

FIGURE 6

The wave function renormalization constant Z_G as a function of κ.

the zero spatial momentum propagator.

$$\frac{1}{L^6}\sum_{\overline{n},\overline{m}}\left\langle \varphi^i_{\overline{n},0}\varphi^k_{\overline{m},t}\right\rangle = G_G(t)\delta^{ik}. \tag{29}$$

Chiral perturbation theory gives the expansion of G_G in powers of $1/L^2$ at fixed t/L and at fixed jL^4

$$G_G(t) = a_G + b_G h(t) + O(1/L^4) \tag{30}$$

where the coefficient b_G is given by

$$b_G = \frac{\Sigma^2}{F_G^2}(1-\eta(u)). \tag{31}$$

The function $h(t)$ is the spatial integral over the propagator associated with the nonzero modes. On the interval $0 < t < L$, it is given by

$$h(t) = \frac{1}{2L^2}\{(\frac{t}{L}-\frac{1}{2})^2 - \frac{1}{12}\}. \tag{32}$$

Numerical data both at finite and zero external field follows rather precisely the predicted parabolic time dependence. The value obtained for Z_G at several κ values are shown in Fig.6. It is interesting to note that Z_G is finite at the critical point $\kappa_c = 0.304(1)$, in fact it is very close to one in the whole investigated region.

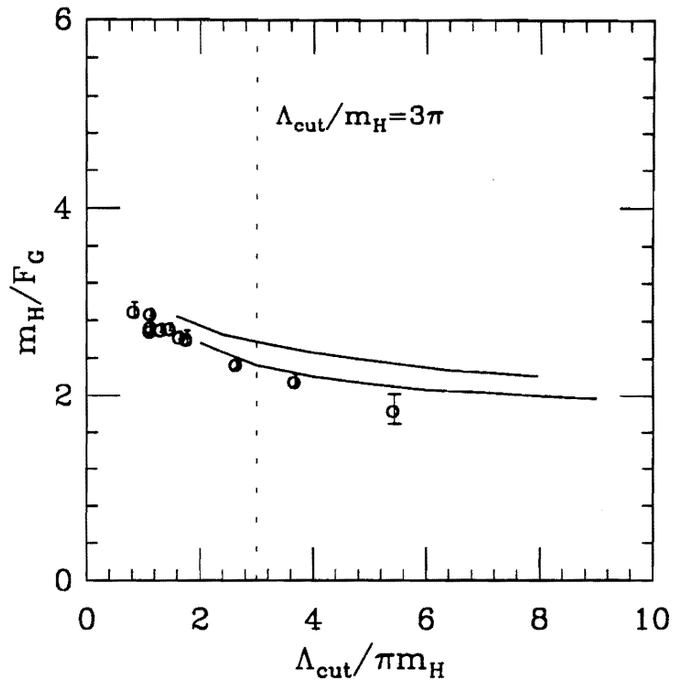

FIGURE 7

Results on the upper bound on hypercubic lattice. The data points are from [16-18], the upper curve is the result of the approximate RG work, the lower curve is from Ref [14].

4.3. Numerical results on the upper bound

Let us collect now the different results on the envelope of m_H/F_G and determine the upper bound for m_H (Fig. 7). The data points from the two large scale collaborations are consistent with each other [16-18]. The analytic results and the approximate RG calculation agrees well with the MC data too. That implies that both the statistical and numerical errors are under control in these works.

The scaling curves for $\langle\sigma\rangle$ and m_R indicates that scaling holds up to $m_H a \approx 0.8$. To be on the safe side we will require $1/m_H a = \Lambda_{cut}/\pi m_H > 3$ which gives the upper bound

$$\begin{aligned} &\frac{m_H}{F_G} \leq 2.6(1), \\ &m_H \leq 8.2(3) m_W \approx 640(25) GeV. \end{aligned} \tag{33}$$

5. Finite cut-off effects on physical amplitudes

The cut-off in an effective theory does not have a precise definition. Physically it signals the energy scale where the theory loses its meaning or where new interactions from some underlying high energy theory become important. Defining the cut-off in a lattice model as π times the inverse lattice spacing is arbitrary; it would be equally correct to set the cut-off twice as large or three times smaller. In a lattice model with not only nearest neighbor but extended interaction terms it is even less obvious how to define the cut-off. It is equally arbitrary to read off the upper bound for the scalar particle in an $O(4)$ scalar model at $m_H/\Lambda_{cut} = 3\pi$ and not at $m_H/\Lambda_{cut} = 10$ or 3. We need a physically controlled way to define the cut-off of an effective theory to fix these arbitrariness.

The finite cut-off in an effective theory has (in principle) calculable effects on physical quantities at lower energies. To make more precise meaning to the Higgs mass upper bound calculations, we should specify the finite cut-off violation effects on definite physical observables instead of fixing the ratio m_H/Λ_{cut} to some arbitrary number. As finite cut-off effects depend on the regularization scheme, this will make it possible to compare different actions, regularizations as well.

In Ref[24] two physically relevant quantities were suggested: the Goldstone-Goldstone scattering cross section at 90° angle at various center of mass energies and the scalar particle width. The finite cut-off effects on these quantities were estimated in the perturbative, weakly coupled region for two regularization schemes, the F4 and hypercubic nearest neighbor lattice regularizations.

The F4 lattice can be obtained from the hypercubic lattice by removing all sites $n = (n_1, n_2, n_3, n_4)$ with $\sum_\mu n_\mu = odd$. The F4 lattice has a higher rotational symmetry than the hypercubic lattice: in 4 dimensions the lattice propagator has no $O(k^4)$ Lorentz invariance breaking term. One would expect less violation of the $O(4)$ symmetry at low momentum and better scaling properties on the F4 than on the hypercubic lattice.

The details of lattice perturbation theory on F4 lattice and the quite involved 1-loop calculation of the Goldstone scattering amplitude and Higgs decay width both on F4 and hypercubic lattices are discussed in Ref[24,25]. The result on the Goldstone scattering is summarized in Fig.8. (Fig.3. of [24]). From the plot one can read off

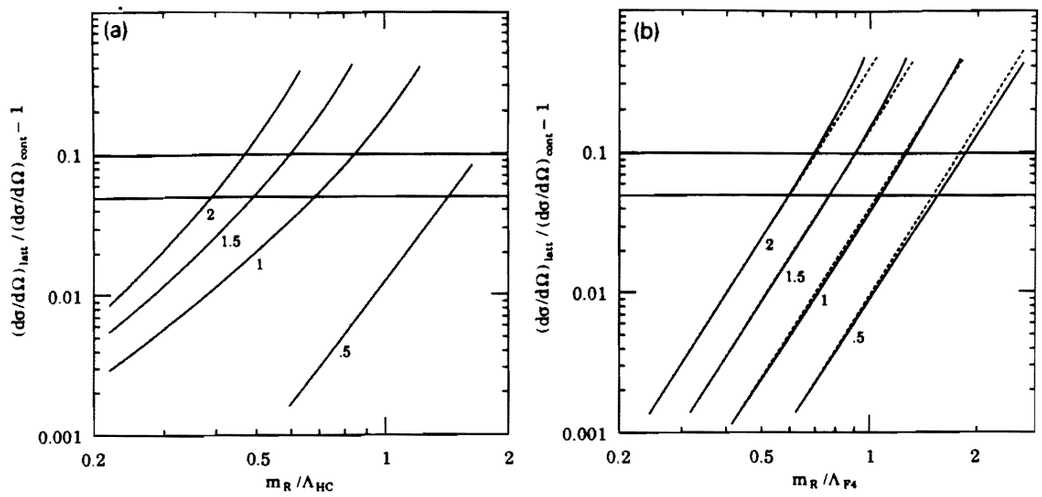

FIGURE 8

Cut-off effect on the cross sections. The lines correspond to c.m. energies W with $W/2m_R = 0.5, 1, 1.5, 2$. The dotted line is the leading term in m_R. The two horizontal lines delimit regions where the cut-off effect is smaller than 10% and 5% respectively. (a) On a hypercubic lattice; (b) on an F_4 lattice.

m_H/Λ_{cut} corresponding to given cut-off effects with given value of the center of mass energy W. The finite cut-off violation is expressed through the ratio of the lattice regularized finite cut-off cross section and the continuum infinite cut-off cross section. For example, a 5% cut-off violation with $W/2m_R = 1.0$ corresponds to $m_H/F_G \approx 1$. on F4 and $m_H/F_G \approx 0.7$ on hypercubic lattice. One can indeed see that on the F4 lattice the same finite cut-off effects allow a larger ratio of m_H/Λ_{cut} than on the hypercubic lattice, the F4 lattice seems to "behave better". (But see the discussion about the definition of Λ_{cut} in the next chapter.)

The cut-off effects on the width of the scalar particle can be expressed in terms of its mass

$$\frac{\Gamma_{latt}}{\Gamma_{cont}} - 1 = \delta(m_R) \tag{34}$$

where

$$\begin{aligned} \delta^{HC} &= \frac{11}{1920} m_R^4 + O(m_R^6), \\ \delta^{F4} &= \frac{1}{240} m_R^4 + O(m_R^6). \end{aligned} \tag{35}$$

From the above formula we obtain that one gets the same cut-off effects on the width

of the scalar particle on the F4 and hypercubic lattices if the masses are related as

$$m_R^{F4} \approx 1.1 m_R^{HC}. \tag{36}$$

In principle similar calculations can be carried out for other regularization schemes making it possible to compare the cut-off effects using well defined physical principles. The calculation is analytically complex and there is no published results other than [24].

One has to note in addition, that the calculation described above is one-loop perturbative. It should be valid as long as the upper bound corresponds to a weakly coupled system, what is the case for both the F4 and hypercubic nearest neighbor actions. However, if one comes up with a regularization scheme predicting a bound outside the perturbative region, some other, non-perturbative method has to be used to compare the scaling violation effects of the new regularization scheme and other schemes.

The finite cut-off effects on the Goldstone-Goldstone scattering or on the width of the Higgs particle provides a physically well defined way to compare different regularization schemes. The drawback of this approach is the involved analytic calculation required, and more importantly, that it works only in the perturbative, weakly coupled regime.

A less physical but perhaps more practical way to compare different schemes is to match their cut-off and compare their scaling behavior. At large cut-off all regularization schemes should show scaling behavior. That means not only a universal functional scaling form for the scalar mass, vacuum expectation value, etc. but the same universal value for the ratio m_H/F_G at the same m_H/Λ_{cut} for different schemes with infinite bare quartic coupling. Λ_{cut} is not a well defined physical quantity, but the cut-off of different regularization schemes can be related by using the above universality. The cut-off scales of different regularizations should be matched in such a way that in the scaling region the ratios m_H/F_G agree. One should see deviation from matching when scaling breaks down for at least one of the regularization schemes. One can set a limit on the scaling violation and compare where different schemes reach that limit. Regularization schemes with "poor" scaling will deviate from the universal curve of m_H/F_G at a smaller m_H/Λ_{cut} value while "good" regularization schemes will follow the scaling curve to large ($\sim O(1)$) m_H/Λ_{cut} values. As m_H/F_G

is monotonically increasing as the function of m_H/Λ_{cut}, the former, "poor" scaling case will predict a lower upper bound for m_H than the latter, "good" scaling case. It might be possible to construct a regularization scheme which does not violate the set scaling behavior even at $m_H \sim \Lambda_{cut}$. It is a different question whether we can be comfortable with the situation where the physical mass is about the same as the cut-off scale where, in a full theory, one expects new interactions to play important roles.

On a hypercubic lattice both m_H and the vacuum expectation value show scaling consistent within statistical errors with the 2-loop perturbative formulae up to $m_H/\Lambda_{cut} \sim 0.8/\pi$. This indicates that the region $m_H/\Lambda_{cut} \sim 1/3\pi$ is well in the scaling region and reading off the upper bound there is rather conservative. That means that all regularization schemes showing scaling at least up to $m_H/\Lambda_{cut} \sim 1/3\pi$ should give the same upper bound $m_H/F_G \leq 2.6(1)$ when the cut-off 3π times larger than the scalar mass assuming the same cut-off is used for the different schemes.

6. Universality

There is no systematic study yet of the universality of the upper bound problem in the $O(4)$ model though several papers dealt with the problem [26-28]. There is a detailed calculation comparing the hypercubic and F4 lattice nearest neighbor action regularization [27]. It uses the physical criteria of fixed (3% and 0.3%) cut-off violation in the Goldstone-Goldstone scattering amplitude to compare the two schemes. Here we just summarize the result, for the details the reader is referred to the original publication.

It turns out that requiring 3% or 0.3% cut-off effects on the scattering amplitude gives a bound for the scalar mass corresponding to a renormalized coupling still in the perturbative regime even for the F4 lattice, therefore the perturbative calculation of Ref[24] as discussed in the previous chapter can be applied. The results for the upper bound corresponding to 3% cut-off effects on the scattering amplitude are

$$\begin{aligned} m_H/F_G &< 590(60) \quad for F4, \\ m_H/F_G &< 640(65) \quad for HC, \end{aligned} \tag{37}$$

and for 0.3% cut-off effects

$$\begin{aligned} m_H/F_G &< 530(60) \quad for F4, \\ m_H/F_G &< 510(50) \quad for HC. \end{aligned} \tag{38}$$

It is somewhat surprising that the F4 lattice bounds are not higher than the hypercubic ones as expected from the better scaling behavior of the F4 scheme. Note however that within errors the ratio values are the same not only for the different regularizations but even for the two different scaling violation limits. One can conclude that with the present numerical accuracy it is not possible to distinguish the cut-off effects on an F4 and hypercubic lattices with nearest neighbor interactions if these effects are required to be less than 3%. Neither it is possible to distinguish, again within numerical accuracy less than 3% cut-off effects of a given regularization.

A more systematic study of the universality was recently presented in Ref[28]. There the analytically solvable spherical $O(n \to \infty)$ model is considered on F4 lattice with actions containing nearest neighbor and next to nearest neighbor terms. In the 2 dimensional parameter space the action giving the largest ratio m_H/F_G at fixed value of m_H/Λ_{cut} was located. The ratio at this point with $m_H\pi/\Lambda_{cut} = 0.5$ is about 30% higher than that of the nearest neighbor action. The authors argue that similar change can be expected in the $O(4)$ model as well.

While it is well possible to obtain a 30% variation in the upper bound by changing the regularization or action, a world of caution is in order here. In Ref[28] the different actions were *not* compared by using the finite cut-off effects on the Goldstone scattering amplitude or similar physical criteria. The 30% change was obtained by comparing the ratios m_H/F_G at the same value of m_H/Λ_{cut} for the different actions. Here the cut-off is defined as $\Lambda_{cut} = \pi/a$, where a is the nearest neighbor lattice spacing. It is not clear that with a large next to nearest neighbor interaction term the inverse lattice spacing has the same physical meaning as with the original nearest neighbor action. In this case it is essential to use a well defined physical criteria to compare the different actions. If one expects an upper bound outside the perturbative region, perturbative calculation of the finite cut-off violation effects on the Goldstone scattering like in Ref[24] will not be sufficient to compare the different actions. Matching their scale and compare scaling behavior is one possibility in addition to a non-perturbative determination of the cut-off violation effects of the Goldstone scattering or other physical quantity.

7. Summary

The Standard Model of electroweak interactions is necessarily an effective theory with a finite cut-off. In an effective theory the Higgs mass, which is a free param-

eter of the model is bounded from above by the requirement that all the low energy particles of the cut-off model should be (much) lighter than the cut-off. The upper bound problem is non-perturbative as it corresponds to infinite bare scalar coupling at the cut-off scale.

In recent years several analytical and numerical studies considered the upper bound problem. The results on nearest neighbor hypercubic lattices are all consistent. The numerical calculations are under control especially those using chiral perturbation theory. The upper bound value on a hypercubic lattice is

$$m_H \leq 640(25) GeV \tag{39}$$

when $m_H \leq \Lambda_{cut}/3\pi$ or the Goldstone scattering amplitude has less then 3% cut-off violation.

The upper bound of the scalar particle is regularization dependent. There is no systematic study considering a whole range of different actions yet. The universality problem has been investigated in depth only for the nearest neighbor F4 and hypercubic lattices in the $O(4)$ model. In these cases the upper bounds turn out to be the same on both lattices within numerical accuracy.

What is the meaning of the Higgs upper bound? First of all it is a bound within the Weinberg-Salam model. It says that the effective Standard Model with finite cut-off cannot describe a Higgs particle heavier than 640GeV if we require that the finite cut-off influence on the Goldstone scattering amplitude is no more than 3%. If the Higgs is heavy, this calculation predicts that the Standard Model model breaks down at a relatively low energy, new interactions have to show up in the few TeV region.

8. References

1) On the present status see for example the plenary talks by J. Ellis and M. Carter at the LP-HEP91 Conference, Geneva, July 1991.

2) K.G. Wilson, Phys. Rev. B4 (1971) 3184;
K.G. Wilson and J. Kogut, Phys. Rep., 12C (1974) 76;
M. Aizenman, Phys. Rev. Lett., 47 (1981) 1; Commun. Math. Phys. 86 (1982) 1;
G.A. Baker and J.M. Kincaid, J. Stat. Phys. 24 (1981) 469;
D.C.. Brydges, J. Fröhlich and T. Spencer, Commun. Math. Phys., 83 (1982) 123;

J. Fröhlich, Nucl. Phys. B200 (1982) 281;
A. D. Sokal, Ann. Inst. H. Poincare A37 (1982) 317;
M. Aizenman and R. Graham, Nucl. Phys. B225 [FS9] (1983) 261;
C. Aragaõ de Carvalho, S. Caracciolo and J. Fröhlich, Nucl. Phys. B215 (1983) 209;
C. B. Lang, Phys. Lett. 155B (1985) 399; Nucl. Phys. B265, FS15 (1986) 630;
see also the last reference of [6].

3) W. A. Bardeen, C. T. Hill, M. Lindner, Phys. Rev. D41 (1990) 1647;
A. Hasenfratz, P. Hasenfratz, K. Jansen, J. Kuti, Y. Shen, Nucl. Phys. B365 (1991) 79.

4) B. W. Lee, C. Quigg, H. Thacker, Phys. Rev. Lett. 38 (1977) 883.

5) The non-perturbative upper bound problem was first formulated in R. Dashen and H. Neuberger, Phys. Rev. Lett. 50 (1983) 1897;
Since then several summary papers have been published in the yearly Lattice Conferences. See
P. Hasenfratz, Nucl. Phys. B (Proc. Suppl.) 9 (1989) 3;
H. Neuberger, Nucl. Phys. B (Proc. Suppl.) 17 (1990) 17;
J. Shigemitsu, Nucl. Phys. B (Proc. Suppl.) 20 (1991) 515.

6) A. Linde, Pisma Zh. Eksp. Teor. Fiz. 23 (1976); JETP Lett. 23 (1976) 64;
S. Weinberg, Phys. Rev. Lett. 36 (1976) 294;
A. Hasenfratz, P. Hasenfratz, Phys. Rev. D34 (1986) 3160.

7) W. Langhuth and I. Montvay, Z. Phys. C36 (1987) 725;
A. Hasenfratz and T. Neuhaus, Nucl. Phys. B297 (1988) 205;
H. G. Evertz, E. Katznelson, P. G. Lauwers, M. Marcu, Phys. Lett. B221 (1989) 143.

8) See for example the second reference in [5].

9) C. Frick, K. Jansen, J. Jersak, I. Montvay, G. Munster, P. Seuferling, Nucl. Phys. B331 (1990) 515;
M. Lüscher, Commun. Math. Phys. 105 (1986) 153.

10) M. Lüscher and P. Weisz, Nucl.Phys. B290[FS20] (1987) 25; Nucl.Phys. B295[FS21] (1988) 65;

11) J. Kuti, L. Lin, Y. Shen Nucl. Phys. B (Proc. Puppl.) 4 (1988) 397; J. Kuti, Y. Shen Phys. Rev. Lett. 60 (1988) 85.

12) P. Hasenfratz and J. Nager, Z. Phys. C37 (1988) 477.

13) A. Hasenfratz, P. Hasenfratz, Nucl. Phys. B270 FS16 (1986) 685.

14) M. Lüscher, P.Weisz, Nucl. Phys. B318 (1989) 705.

15) M.M. Tsypin Lebedev Physical Inst. Pr. 280 (1985).

16) A. Hasenfratz, T. Neuhaus, K. Jansen, Y. Yoneyama and C. B. Lang, Phys. Lett. 199B (1987) 531;

A. Hasenfratz, K. Jansen, J.Jersak,T. Neuhaus, C. B. Lang and Y. Yoneyama, Nucl. Phys. B317 (1989) 81.

17) J. Kuti,L. Lin, Y. Shen, Nucl. Phys. B (Proc. Suppl.) 9 (1989) 26.

18) A. Hasenfratz, K. Jansen, J.Jersak, C. B. Lang, H. Leutwyler,T. Neuhaus, Z. Phys. C46 (1990) 257; Nucl. Phys. B356 (1991) 332.

19) M. Göckeler , K.Jansen, T. Neuhaus, preprint UCSD/PTH 91-15.

20) H. Leutwyler, Nucl. Phys. B (Proc. Suppl.) 4 (1988) 248;
P. Hasenfratz and H. Leutwyler, Nucl. Phys. B343 (1990) 241.

21) H. Neuberger, Phys. Rev. Lett. 60 (1988) 889; Nucl. Phys. B300 FS22 (1988);
U.M.Heller, H. Neuberger, Phys. Lett. B207 (1988) 189.

22) M. Gockeler, H. Leutwyler, Nucl. Phys. B350 (1991) 228; Phys. Lett. B253 (1991) 193.

23) J. Gasser and H. Leutwyler, Phys. Lett. B184 (1987) 83; Phys. Lett. B188 (1987) 477; Phys. Lett. B189 (1987) 197; Nucl. Phys. B307 (1988) 763;

24) G. Bhanot, K. Bitar, U.M. Heller, H. Neuberger, Nucl. Phys. B343 (1990) 467.

25) H. Neuberger, Phys. Lett. B199 (1987) 536.

26) G. Bhanot, K. Bitar,Phys. Rev. Lett. 61 (1988) 798;
C.B.Lang, Phys. Lett. B229 (1989) 97.

27) G. Bhanot, K. Bitar, U.M. Heller, H. Neuberger, Nucl. Phys. B353 (1991) 551.

28) U.M. Heller, H. Neuberger, P. Vranas, preprint FSU-SCRI-91-94, (1991)